



## 2-Aminothiadiazoles inhibitors of AKT1 as potential cancer therapeutics

Qingping Zeng<sup>a</sup>, Matthew P. Bourbeau<sup>a,\*</sup>, G. Erich Wohlhieter<sup>a</sup>, Guomin Yao<sup>a</sup>, Holger Monenschein<sup>a</sup>, James T. Rider<sup>a</sup>, Matthew R. Lee<sup>a</sup>, Shiwen Zhang<sup>b</sup>, Julie Lofgren<sup>b</sup>, Daniel Freeman<sup>b</sup>, Chun Li<sup>c</sup>, Elizabeth Tominey<sup>c</sup>, Xin Huang<sup>d</sup>, Douglas Hoffman<sup>e</sup>, Harvey Yamane<sup>f</sup>, Andrew S. Tasker<sup>a</sup>, Celia Dominguez<sup>a</sup>, Vellarkad N. Viswanadhan<sup>a</sup>, Randall Hungate<sup>a</sup>, Xiaoling Zhang<sup>b</sup>

<sup>a</sup> Chemistry Research and Discovery, Amgen Inc., One Amgen Center Drive, Thousand Oaks, CA 91320, USA

<sup>b</sup> Oncology Research, Amgen Inc., One Amgen Center Drive, Thousand Oaks, CA 91320, USA

<sup>c</sup> Pharmacokinetics and Drug Metabolism, Amgen Inc., One Amgen Center Drive, Thousand Oaks, CA 91320, USA

<sup>d</sup> Chemistry Research and Discovery, Amgen, Inc., 1 Kendall Square, Cambridge, MA 02139, USA

<sup>e</sup> Small Molecule Process and Product Development, Amgen Inc., One Amgen Center Drive, Thousand Oaks, CA 91320, USA

<sup>f</sup> Protein Science, Amgen Inc., One Amgen Center Drive, Thousand Oaks, CA 91320, USA

### ARTICLE INFO

#### Article history:

Received 19 December 2009

Revised 8 January 2010

Accepted 11 January 2010

Available online 20 January 2010

### ABSTRACT

A series of 2-aminothiadiazoles of inhibitors of AKT1 is described. SAR relationships are discussed, along with selectivity for protein kinase A (PKA) and cyclin-dependent kinase 2 (CDK2). Moderate selectivity observed in several compounds for AKT1 versus PKA is rationalized by X-ray crystallographic analysis. Key compounds showed activity in cellular assays measuring phosphorylation of two AKT substrates, PRAS40 and FKHL1. Compound **30** was advanced to a mouse liver PD assay, where it showed dose-dependent inhibition of AKT activity, as measured by the inhibition of phospho-PRAS40.

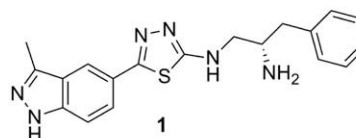
© 2010 Elsevier Ltd. All rights reserved.

The serine/threonine kinase AKT (also named protein kinase B, or PKB) is a key component in the signaling cascades mediated by growth factor receptors and one of the most frequently activated protein kinases in a number of human cancers.<sup>1–3</sup> Constitutively activated AKT provides a driving factor for tumor growth and survival, and is associated with the resistance of many cancers to current therapies. There are three AKT isoforms in mammalian cells (AKT1/PKB $\alpha$ , AKT2/PKB $\beta$ , and AKT3/PKB $\gamma$ ), which have shown both distinct and overlapping functions in normal physiology. All three isoforms possess the transforming ability important for tumor formation, although arising data has suggested AKT1 is the major isoform contributing to the oncogenic activity.<sup>2</sup> Various groups have pursued AKT1 inhibitors as a promising anti-cancer therapy with the potential for broad application in areas including ovarian, breast, and prostate cancers.<sup>4,5</sup>

We have undertaken a research program with the goal of developing an AKT1 inhibitor for the treatment of human cancers. Our work in this area has focused on a chemical series of 5-aminothiadiazoles, exemplified by rationally designed lead compound **1** (Fig. 1). In addition to AKT, compound **1** was found to inhibit protein kinase A (PKA) and cyclin-dependent kinase 2 (CDK2). We followed PKA and CDK2 selectivity as we developed the 2-aminothiadiazoles series. PKA is highly homologous to AKT in the kinase domain and is a prototype for the ACG kinase family. It was expected that improved selectivity for PKA might lead to more broadly improved

kinase selectivity.<sup>6</sup> CDK2 is a serine/threonine kinase that regulates cell cycle transition and cell proliferation.<sup>7</sup> To understand desired selectivity against these kinases, we followed PKA and CDK2 activity for all subsequent compounds synthesized. This Letter details the SAR explorations that resulted in the discovery of compounds with improved enzymatic potency relative to **1**. Select compounds also showed activity in cellular and pharmacodynamic studies.

The general synthetic approach used for indazole containing compounds in this Letter is shown in Scheme 1. In order to prepare 3-substituted indazoles, aldehyde **2** was treated with the appropriate alkyl or aryl Grignard reagent (RMgBr) and the resulting alcohol was oxidized to ketones **3**. Reaction of ketones **3** with hydrazine afforded the corresponding indazoles **4**. In the case of unsubstituted indazoles (R = H), steps a and b were omitted and **2** was treated with hydrazine directly (step c). Lithiation, followed by quenching with

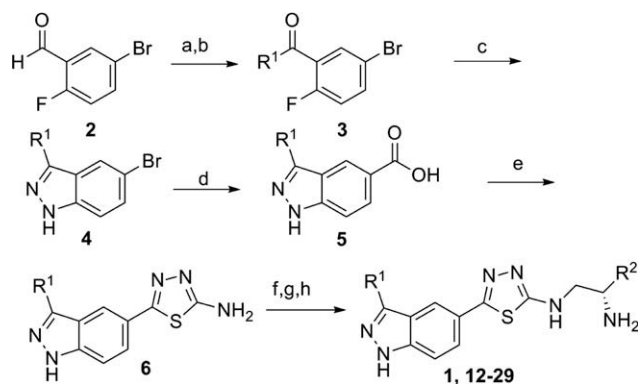


AKT1 IC <sub>50</sub> (nM)	PKA IC <sub>50</sub> (nM)	CDK2 IC <sub>50</sub> (nM)
76 ± 19	54 ± 12	72 ± 14

**Figure 1.** Original lead compound in thiadiazoles series. Data is reported as the mean ± SD where n ≥ 3.

\* Corresponding author.

E-mail address: [bourbeau@amgen.com](mailto:bourbeau@amgen.com) (M.P. Bourbeau).



**Scheme 1.** Synthesis of **1**, **12–29**. Reagents and conditions: (a) RMgBr, THF, 0 °C, 89–100%; (b) PDC, molecular sieves, CH<sub>2</sub>Cl<sub>2</sub>, 25–84%; (c) hydrazine, 117 °C, 65–94%; (d) *t*-BuLi, THF, then CO<sub>2</sub>, 31–94%; (e) PPA, thiosemicarbazide, 90 °C, 53–92%; (f) *N*-Boc amino acids, EDCI, HOBT, DMF; (g) LiAlH<sub>4</sub>, THF, 0 °C to rt; (h) TFA, CH<sub>2</sub>Cl<sub>2</sub>, 5–10% for three steps.

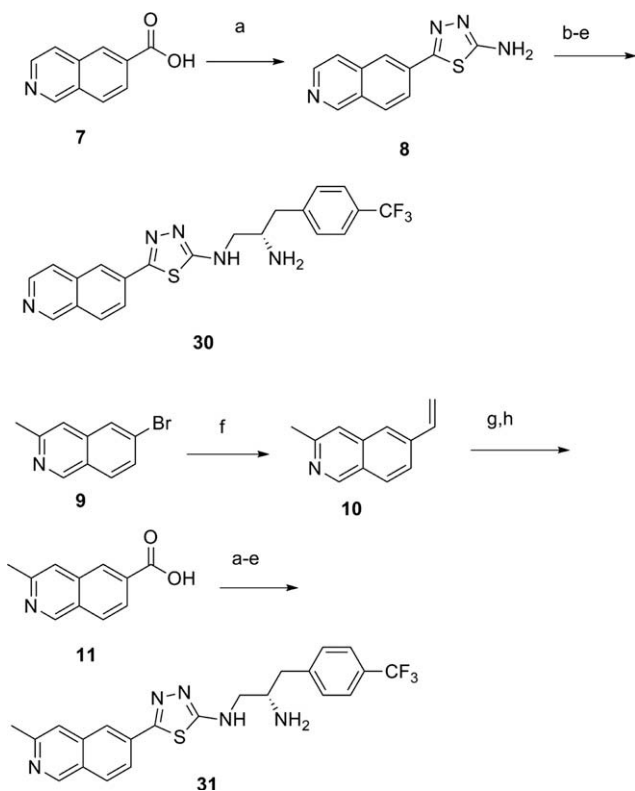
CO<sub>2</sub>, led to carboxylic acids **5**. Conversion to 5-aminothiadiazoles **6** was followed by amide coupling with a commercially available *N*-Boc protected amino acid. The resulting amides were reduced using LiAlH<sub>4</sub>. TFA deprotection of the primary amine afforded the desired products **1**, **12–29**.

A similar approach used to synthesize isoquinoline containing compounds **30** and **31** is outlined in Scheme 2. Commercially available carboxylic acid **7** was converted to thiadiazole **8** by treatment with thiosemicarbazide in polyphosphoric acid. The thiadiazole was coupled with *N*-Boc (*S*)-2-amino-3-(4-(trifluoromethyl)ph-

enyl)propanoic acid, and the resulting amide was reduced with LiAlH<sub>4</sub>. This resulted in partial over-reduction of the isoquinoline, so the product was treated with palladium on carbon in cyclohexene to oxidize the over reduced product. Treatment with TFA then afforded isoquinoline **30**. 6-Bromo-3-methylisoquinoline was prepared via published methods<sup>8</sup> and coupled with vinyltributyltin to afford olefin **10**. The olefin was subjected to ozonolysis followed by oxidation of the resulting aldehyde to the corresponding carboxylic acid **11**. Following steps a–e, the acid was then converted to diamine **31**.

Utilizing the amino acid coupling described in Scheme 1, we were able to rapidly examine changes to the diamino portion of the molecule (Table 1).<sup>9,10</sup> To establish the preferred stereochemistry of the chiral amine, the *R*-enantiomer of **1** (**R-1**) was synthesized and found to be less potent in the AKT1 enzymatic assay than the *S* enantiomer. We next examined whether introducing substitutions on the phenyl ring might improve potency. Commercially available *S*-phenylalanine analogs were used as inputs. Substitution at the 2 position of the ring with F, Cl, or CF<sub>3</sub> led to compounds with similar or reduced potency compared to **1** (**12–14**), and with no selectivity over PKA. In contrast, substitution at the 3 and 4 positions with F, Cl, or CF<sub>3</sub> was found to generally enhance potency and, in the case of **17–19**, resulted in compounds that inhibited AKT1 activity with IC<sub>50</sub> values in the single digit nanomolar range. This improvement in activity could be rationalized by X-ray crystal structure analysis of several key compounds (see below). We also synthesized two examples with disubstitution on the phenyl ring (**20** and **21**). These compounds also showed increased enzymatic potency relative to **1**, but they were not as potent as the best monosubstituted examples (i.e., **19**). No significant selectivity for PKA or CDK2 was observed in any compound.

Having shown potency could be improved by changes to the amino phenyl portion of **1**, we next examined changes to the 3-position of the indazole ring (Table 2). Replacement of the methyl group with larger groups (**22–24**) resulted in a loss of potency relative to **1**. However, if the methyl group was replaced with a hydrogen, potency was maintained in most cases (**25**, **27–29**). In addition to retaining potency, several of these compounds began to show modest selectivity over PKA. Compound **28**, in particular, showed 20-fold selectivity over PKA. Compounds **28** and **29** also showed modest selectivity for CDK2 (4–8-fold).



**Scheme 2.** Synthesis of **30** and **31**. Reagents and conditions: (a) PPA, thiosemicarbazide, 90 °C, 59–76%; (b) *N*-Boc (*S*)-2-amino-3-(4-(trifluoromethyl) phenyl)propanoic acid, EDCI, HOBT, DIEA, DMF; (c) LiAlH<sub>4</sub>, THF, 0 °C; (d) Pd/carbon, 10%, cyclohexene; (e) TFA, DCM, 2–11% for four steps; (f) vinyltributyltin, Pd(PPh<sub>3</sub>)<sub>4</sub>, dioxane, 92%; (g) O<sub>3</sub>, DMS/NaHCO<sub>3</sub>, 7:1 MeOH/DCM, 88%; (h) NaClO<sub>2</sub>, NaH<sub>2</sub>PO<sub>4</sub>·H<sub>2</sub>O, 2-methyl-2-butene, *t*-BuOH/H<sub>2</sub>O, 53%.

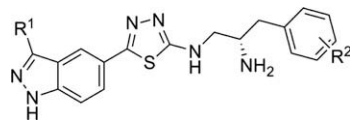
**Table 1**  
SAR of changes to the phenyl ring of compound **1**

Compds	R	AKT1 IC <sub>50</sub> (nM)	PKA IC <sub>50</sub> (nM)	CDK2 IC <sub>50</sub> (nM)
<b>1</b>	H	76 ± 12	54 ± 12	72 ± 14
<b>R-1</b>	H	>2200 <sup>a</sup>	NT <sup>b</sup>	NT <sup>b</sup>
<b>12</b>	2-F	198 ± 10	215 ± 150	104 <sup>a</sup>
<b>13</b>	2-Cl	47 ± 7	106 ± 39	57 ± 14
<b>14</b>	2-CF <sub>3</sub>	491 ± 35	247 ± 40	198 ± 96
<b>15</b>	3-F	38 ± 6	230 ± 190	NT <sup>b</sup>
<b>16</b>	3-Cl	19 ± 0.2	15 ± 4	17 ± 2
<b>17</b>	3-CF <sub>3</sub>	6.1 ± 0.1	6.5 ± 2	35 ± 22
<b>18</b>	4-Cl	8.9 ± 2	11 ± 2	72 ± 47
<b>19</b>	4-CF <sub>3</sub>	5.5 ± 0.1	13 ± 4	17 ± 6
<b>20</b>	2,4-Dichloro	18 ± 4	43 ± 28	70 ± 7
<b>21</b>	3,4-Difluoro	14 ± 3	27 ± 21	19 ± 6

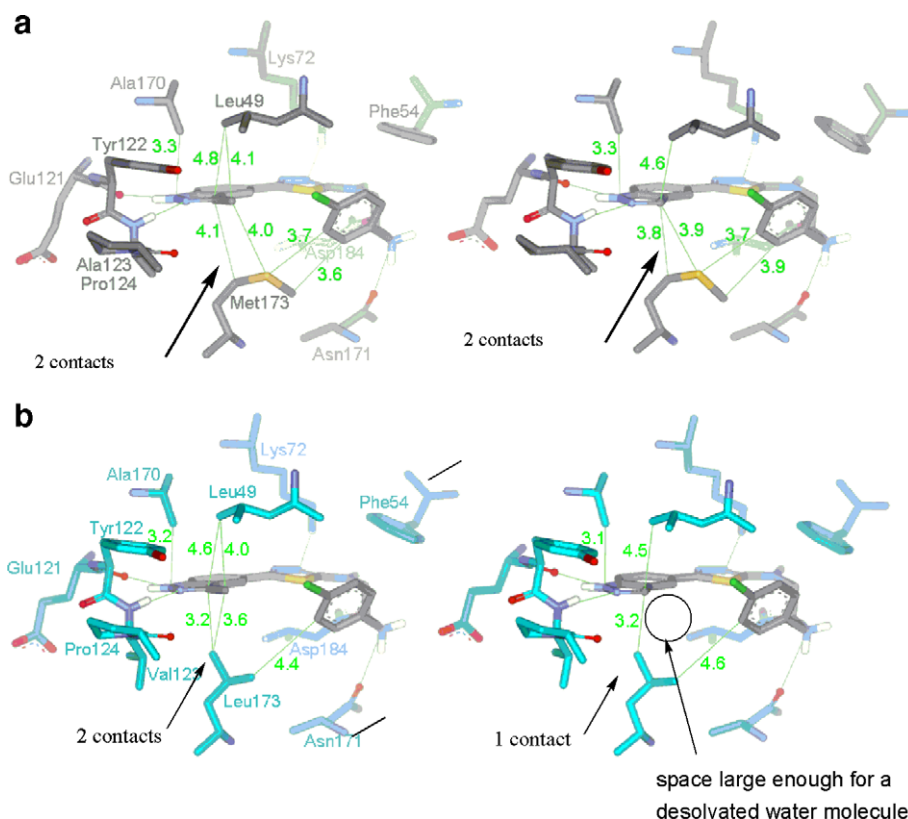
Data reported as the mean ± SD where *n* ≥ 3 except (a) tested once; (b) NT = not tested.

**Table 2**

The effect of changes in the substitution at the 3 position of the indazole



Compound	R <sup>1</sup>	R <sup>2</sup>	AKT1 IC <sub>50</sub> (nM)	PKA IC <sub>50</sub> (nM)	CDK2 IC <sub>50</sub> (nM)
<b>1</b>	Me	H	76 ± 19	54 ± 12	72 ± 14
<b>22</b>	Et	H	370 <sup>a</sup>	NT <sup>b</sup>	NT <sup>b</sup>
<b>23</b>	Cyclopropyl	4-CF <sub>3</sub>	181 ± 24	237 ± 60	135 ± 115
<b>24</b>	Phenyl	3-CF <sub>3</sub>	413 ± 20	368 ± 86	79 ± 7
<b>25</b>	H	3-CF <sub>3</sub>	25 ± 1	117 ± 33	NT <sup>b</sup>
<b>26</b>	H	4-F	368 ± 8	373 ± 93	74 ± 12
<b>27</b>	H	4-Cl	24 ± 4	157 ± 56	41 ± 26
<b>28</b>	H	4-CF <sub>3</sub>	6.0 ± 1	108 ± 15	24 ± 8
<b>29</b>	H	2,4-Dichloro	40 ± 7	158 ± 88	323 <sup>a</sup>

Data reported as the mean ± SD where *n* ≥ 3 except (a) tested once; (b) NT = not tested.**Figure 2.** (a) X-ray crystal structures of **18** and **27** with PKA triple mutant designed to mimic the active site of AKT. (b) Model of **18** and **27** docked into the PKA active site.

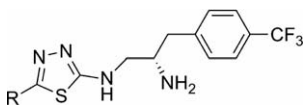
We were able to obtain X-ray co-crystal structures of several compounds with a triple-mutant construct of PKA's kinase domain that mimics the ATP binding pocket of AKT (Fig. 2, residue numbering is based on PKA).<sup>11–14</sup> These compounds were observed to bind in a 'U' shaped manner with the indazole, forming two hydrogen bonds with the amino acid strand that links the N-terminal and C-terminal domains (often referred to as the linker strand or hinge region), consisting of a hydrogen bond acceptor to the backbone NH of Ala123 and a hydrogen bond donor to the backbone carbonyl O of Glu121. The thiadiazole acted as a hydrogen bond acceptor for the catalytic Lys72, which is essential for ATP hydrolysis. The primary amine formed a salt bridge with Asp184 (not displayed in Fig. 2) and also a hydrogen bond with the amide sidechain of

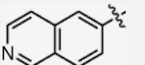
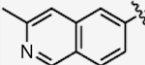
Asn171. The phenyl ring of the diamine sidechain folded back towards the indazole, forming an edge-to-face contact with the thiadiazole. Substitutions at C3 and C4 of the diamino sidechain phenyl ring (**15–21**) appeared to further stabilize the U-shape through intramolecular Van der Waals contacts with the indazole and improved contacts with residues Met173, Phe327, Leu49, and Val57. The phenyl ring also formed intermolecular hydrophobic contacts with Met173 and Glu127 (not shown). A structurally similar series has been reported to bind in a slightly different, 'Z' shaped conformation in the PKA triple mutant.<sup>14</sup>

Careful analysis of crystal structures of **18** and **27** with the PKA triple mutant, as well as modeling of the two compounds docked<sup>15</sup> into the wild type PKA active site, indicated a subtle difference in

**Table 3**

The effect of changes in the substitution of the phenyl ring of the indazole



Compound	R	AKT <sub>1</sub> IC <sub>50</sub> (nM)	PKA IC <sub>50</sub> (nM)	CDK <sub>2</sub> IC <sub>50</sub> (nM)
<b>30</b>		3 ± 0.1	8 ± 17	53 ± 23
<b>31</b>		280 ± 40	274 ± 15	607 ± 15

Data reported as ±SD where  $n \geq 3$ .

the interaction with a key amino acid (the 'floor residue', Met173 in the PKA triple mutant and Leu173 in PKA) that offered a rationale for the kinase selectivity difference observed between **18** and **27**. In the triple-mutant crystal structure, the indazole of **18** makes two key hydrophobic contacts with Met173 (Fig. 2a). In the case of **27**, the crystallographic structures demonstrated that Met173 was able to slightly reorient its sidechain to accommodate the space vacated by the removal of the methyl group at the 3-position of the indazole, thereby maintaining hydrophobic contacts with the indazole of **27**. When these compounds were docked into wild type PKA, the indazole of compound **18** was also predicted to make two hydrophobic contacts with one of the delta carbons of Leu173 (Fig. 2b). However, according to the model of **27**, Leu173 was only able to maintain one of the hydrophobic interactions with the indazole, which likely results from the gamma branching of the leucine and one less rotatable bond compared to the methionine in AKT. This net loss of one key hydrophobic interaction in PKA likely accounted for much of the 10–20-fold difference in potency observed for compounds lacking the indazole methyl group, such as **27**. Another cause of the loss of PKA activity in the 3-H indazoles may be that the added space allowed for a single water molecule to be trapped and desolvated from bulk solvent thereby leading to an entropic penalty. Differences in the Leu173/Met173 interactions have been previously implicated in AKT/PKA selectivity observed in other chemical series, although the structurally based rational for the observed selectivity was different.<sup>11,14</sup>

In addition to compounds featuring an indazole head group, we also explored the replacement of the indazole with an isoquinoline, synthesized as outlined in Scheme 2. Compound **30** showed AKT1 potency similar to indazoles such as **19**, but no selectivity over PKA (Table 3). This lack of selectivity over PKA could be explained by the isoquinoline occupying a similar volume in the active site as the 3-methyl indazole, also maintaining two hydrophobic contacts with the floor residues in both AKT1 and PKA. Methylation at the 3 position of the isoquinoline led to a nearly 100 loss in potency (**31**), possibly due to disruption of the U-shaped interaction by the methyl group. Interestingly, **30** showed improved selectivity over CDK2 (~20-fold).

**Table 4**Enzymatic, cellular activity, and PK data for **19**, **28**, and **30**

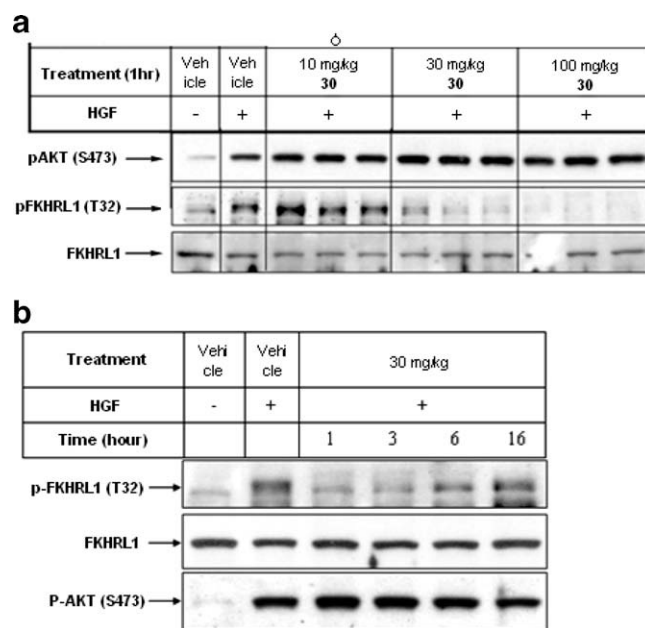
Compound	AKT enzymatic IC <sub>50</sub> (nM)	pPRAS40 cellular IC <sub>50</sub> (nM)	pFKHRL1 cellular IC <sub>50</sub>	CL (L/h/kg) iv	T <sub>1/2</sub> (h) iv	V <sub>ss</sub> (L/kg) iv	C <sub>max</sub> (ng/mL) po	%F po
<b>19</b>	5.5 ± 0.1	357 ± 180	333 ± 39	2.8	4.1	13.7		
<b>28</b>	6.0 ± 1	444 ± 197	154 <sup>a</sup>	4.9	2.5	13.3		
<b>30</b>	3.2 ± 0.07	247 ± 107	695 ± 125	1.5	3.8	3.8	430	20

Enzyme and cell data reported as the mean ± SD where  $n \geq 3$  except (a) tested once.

Several of the more potent compounds were then profiled in cell-based assays and rat pharmacokinetics (PK) studies (Table 4). Two cellular assays were utilized; the first assay measured phosphorylation of PRAS40 (Thr246) in U87MG cells via an enzyme-linked immunosorbent assay (ELISA).<sup>16,17</sup> The second assay measured the translocation of FKHRL1 in a cell immunoassay.<sup>18,19</sup> Both PRAS40 and FKHRL1 have been shown to be direct substrates of AKT. All of the compounds showed activities in the two cellular assays, although cellular potency was much lower than enzymatic potency (30–200-fold lower). This shift in potency was not directly correlated with protein binding, permeability, or solubility (data not shown). Additionally, compound **30** was found to inhibit cellular proliferation in U87MG cells (EC<sub>50</sub> = 380 ± 150 nM), which correlates with the inhibition of PRAS40 and FKHRL1 phosphorylation.<sup>20</sup>

The compounds were tested in a rat iv PK study.<sup>21</sup> Compounds **19** and **28** showed high clearance and high volumes of distribution (>13 L/kg), with half lives of 4.1 and 2.5 h, respectively. Compound **30**, on the other hand, showed a moderate clearance (1.5 L/h/kg, approximately half of rat hepatic blood flow), low volume of distribution, and reasonable oral bioavailability (20%).

We advanced **30** to a mouse liver pharmacodynamic (PD) assay. This assay measures phospho-FKHRL1 levels in mouse livers stimulated with exogenously administered hepatocyte growth factor (HGF).<sup>22</sup> Inhibition of phospho-FKHRL1 was measured at 1 h after treatment in the 30 and 100 mg/kg dose groups (Fig. 3a), and the effect was dose dependent. There was no reduction in phospho-AKT<sup>23</sup> levels (which is stimulated by HGF), suggesting that the inhibition of phospho-FKHRL1 was a result of the inhibition of

**Figure 3.** (a) Dose–response PD study with **30** measuring inhibition of phosphor-FKHRL1. (b) Time course PD study of **30** measuring phosphor-FKHRL1 at 30 mg/kg.



AKT itself and not inhibition of an upstream kinase. FKHRL1 has also been shown to be phosphorylated at T32 by the SGK kinases.<sup>24</sup> Compound **30** was tested in an SGK1 enzymatic assay,<sup>25</sup> and was found to be ~700-fold less potent on SGK1 than AKT1 (SGK1 IC<sub>50</sub> 2.2 ± 0.6 μM). This further suggested that the inhibition of phospho-FKHRL1 was driven by AKT inhibition. The PD effect was then examined in a time course study.<sup>26</sup> At 30 mg/kg, compound **30** showed effective inhibition of phospho-FKHRL1 at 1, 3, and 6 h post-dose (Fig. 3b). Again, there was no reduction in phospho-AKT levels in this study.

In conclusion, a series of AKT1 inhibitors is described. SAR studies resulted in compounds with enzymatic inhibition of AKT1 at single digit nanomolar IC<sub>50</sub> values. In some cases, modest selectivity over PKA was achieved. The origin of this selectivity can be rationalized by X-ray crystallographic analysis. Key compounds showed inhibition of AKT cellular activity as measured by the inhibition of phosphorylation of AKT substrates PRAS 40 and FKHRL1. Compound **30** had favorable rat PK and in mouse liver PD studies, showed effective inhibition of phospho-FKHRL1 at 30 mg/kg for up to 6 h post-dose.

## Acknowledgements

The authors are indebted to John Allen, Christopher Fotsch, and Isabelle Dussault for their critical review of this Letter.

## References and notes

- Luo, J.; Manning, B. D.; Cantley, L. C. *Cancer Cell* **2003**, 4, 20.
- Dummler, B.; Hemmings, B. A. *Biochem. Soc. Trans.* **2007**, 35, 231.
- LoPiccolo, J.; Granville, C. A.; Gills, J. J.; Dennis, P. A. *Anti-Cancer Drugs* **2007**, 18, 861.
- Li, Q. *Expert Opin. Ther. Pat.* **2007**, 17, 1077.
- Heerding, D. A.; Safonov, I. G.; Verma, S. K. *Annu. Rep. Med. Chem.* **2008**, 42, 365.
- Johnson, D. A.; Akamine, P.; Radzio-Andzelm, E.; Madhusudan; Taylor, S. S. *Chem. Rev.* **2001**, 101, 2243.
- Besson, A.; Dowdy, S. F.; Roberts, J. M. *Dev. Cell.* **2008**, 14, 159.
- Miller, R. B.; Frincke, J. M. *J. Org. Chem.* **1980**, 45, 5312.
- AKT1, PKA, SGK1, and CDK2 enzymatic activity was measured using a previously described method.<sup>25</sup> The ATP concentrations were 10 μM for all kinase reactions. Cyclin 2E was used as the cyclin partner for the CDK2 assay.
- All compounds were characterized by NMR and MS, and were >95% pure by HPLC.
- Mutations: PKA Val123 was mutated to AKT Ala, and PKA Leu173 was mutated to AKT Met. Additionally, PKA Lys181 was mutated to AKT Gln, but this residue faces away from the ATP binding pocket. For a description of a similar crystallography strategy see: Caldwell, J. J.; Davies, T. G.; Donald, A.; McHardy, T.; Rowlands, M. G.; Aherne, G. W.; Hunter, L. K.; Taylor, K.; Ruddle, R.; Raynaud, F. I.; Verdonk, M.; Workman, P.; Garrett, M. D.; Collins, I. *J. Med. Chem.* **2008**, 51, 2147.
- The coordinates for the co-crystal structures of **18** and **27** have been deposited with the RSCB and PDB. **18**: RCSB ID code RCSB057006, PDB ID code 3L9M. **27**: RCSB ID code RCSB057007, PDB ID code 3L9N.
- Gaßel, M.; Breitenlechner, C. B.; Rüger, P.; Jucknischke, U.; Schneider, T.; Huber, R.; Bossemeyer, D.; Engh, R. A. *J. Mol. Biol.* **2003**, 329, 1021.
- Davies, T. D.; Verdonk, M. L.; Graham, B.; Saalau-Bethell, S.; Hamlett, C. C. F.; McHardy, T.; Collins, I.; Garrett, M. D.; Workman, P.; Woodhead, S. J.; Jhoti, H.; Barford, D. *J. Mol. Biol.* **2007**, 367, 882.
- Lee, M. R.; Sun, Y. *J. Chem. Theo. Comp.* **2007**, 3, 1106.
- U87MG cells in 5% FBS media were incubated with inhibitors in threefold serial dilutions for 1 h at 37 °C. The cells were lysed and PRAS40 phosphorylation was quantified by ELISA assay. Phospho-PRAS40 was normalized to total PRAS40.
- Kovacina, K. S.; Park, G. Y.; Bae, S. S.; Guzzetta, A. W.; Schaefer, E.; Birnbaum, M. J.; Roth, R. A. *J. Biol. Chem.* **2003**, 278, 10189.
- FKHRL1 nuclear translocation was measured in MDA-MB-468 cells stably expressing a fluorescence-tagged FKHRL1 fusion protein (FKHRL-GFP). Cells were treated in threefold serial dilutions of test compounds and nuclear translocation was evaluated by fluorescence microscopy.
- Brunet, A.; Bonni, A.; Zigmond, M. J.; Lin, M. Z.; Juo, P.; Hu, L. S.; Anderson, M. J.; Arden, K. C.; Blenis, J.; Greenberg, M. E. *Cell* **1999**, 96, 857.
- U-87 glioblastoma cells were seeded on 96-well cell culture plate at 6000 cells/well, and treated with compounds at indicated concentrations for 3 days. Cell viability was measured by alamarBlue® cell staining (Invitrogen, DAL1100). The assay was run in triplicate.
- Compounds were dosed in *n* = 3 male Sprague/Dawley rats. iv dosing: 1 mg/kg in 100% DMSO for **19** and **28**. 2 mg/kg in 100% DMSO for **30**. po dosing: 10 mg/kg 25% PEG 400/5% water for **30**.
- Balb/c female mice (*n* = 3) were dosed with compounds **30** (ip, 25% PEG400, 75% H<sub>2</sub>O). 1 h post-dose, AKT signaling was stimulated in mouse liver by hepatocyte growth factor (HGF) via tail vein injection (5 μg). Five minutes post HGF stimulation, the mice were sacrificed and livers were harvested for protein lysate preparation and quantitation by Western blot analysis of phospho-FKHRL1 (Thr32), normalized to total FKHRL1 levels.
- The phospho-AKT specific antibody detects all three isoforms.
- Brunet, A.; Park, J.; Tran, H.; Hu, L. S.; Hemmings, B. A.; Greenberg, M. E. *Mol. Cell. Biol.* **2001**, 21, 952.
- Zhang, X. L.; Zhang, S. W.; Yamane, H.; Wahl, R.; Ali, A.; Lofgren, J. A.; Kendall, R. L. *J. Biol. Chem.* **2006**, 281, 13949.
- Balb/c female mice (*n* = 3) were dosed with compounds **30** (ip, 25% PEG400, 75% H<sub>2</sub>O). 1, 3, 6, or 16 h post-dose, AKT signaling was stimulated in mouse liver by hepatocyte growth factor (HGF) via tail vein injection (5 μg). Five minutes post HGF stimulation, the mice were sacrificed and livers were harvested for protein lysate preparation and quantitation by Western blot analysis of phospho-FKHRL1 (Thr32), normalized to total FKHRL1 levels.